J. Hydrol. Hydromech., *60*, 2012, 4, 288–298
DOI: 10.2478/v10098-012-0025-0

ZONE OF FLOW SEPARATION AT THE UPSTREAM EDGE OF A RECTANGULAR BROAD-CRESTED WEIR

ZBYNĚK ZACHOVAL, IVANA MISTROVÁ, LADISLAV ROUŠAR, JAN ŠULC, PAVEL ZUBÍK

Brno University of Technology, Faculty of Civil Engineering, Institute of Water Structures, Veveří 95, 602 00 Brno, Czech Republic; Mailto: zachoval.z@fce.vutbr.cz

The paper deals with the determination of the basic characteristics of flow at the crest of a rectangular broad-crested weir and in detail with the characteristics of flow separation at the upstream edge of the weir crest. The determination of the characteristics is made on the basis of measurement of the water surface level, the pressure head and the velocity field using the Particle Image Velocimetry method. The characteristics are expressed dimensionless in relation to the energy overflow head and the critical depth.

KEY WORDS: Rectangular Broad-Crested Weir, Separation Zone, Separated Flow.

Zbyněk Zachoval, Ivana Mistrová, Ladislav Roušar, Jan Šulc, Pavel Zubík: OBLAST ODTRŽENÍ PROUDU NA NÁVODNÍ HRANĚ PRAVOÚHLÉHO PŘELIVU SE ŠIROKOU KORUNOU. J. Hydrol. Hydromech., *60*, 2012, 4; 21 lit., 6 obr.

Článek pojednává o stanovení základních charakteristik proudu na široké koruně pravoúhlého přelivu a detailně o charakteristikách odtržení proudu za návodní hranou koruny přelivu. Charakteristiky jsou stanoveny na základě měření úrovně hladiny, tlakové výšky a rychlostního pole metodou Particle Image Velocimetry. Charakteristiky jsou vyjádřeny bezrozměrně ve vztahu k energetické přepadové výšce a kritické hloubce.

KLÍČOVÁ SLOVA: pravoúhlý přeliv se širokou korunou, oblast odtržení, odtržený proud.

Introduction

Broad-crested weirs are very often used in water management as, e.g., measuring weirs (*Boiten*, 2002), fixed weirs and lateral weirs. Their advantages are the robustness of construction, a simple shape, easy maintenance, etc. (*USBR*, 2001). Broad-crested weirs are rectangular in cross section (Fig. 1) (*ČSN ISO 3846*, 1994) or non-rectangular. Rectangular weirs have a horizontal crest with the width t, and the upstream and downstream walls are vertical with sharp edges. They are manufactured from plastics, metals, concrete, wood, etc. (*Clemmens* et al., 2001).

During overflowing a rectangular weir (Fig. 1), three zones of flow separation are created (*Hager*, 1986). The first zone of flow separation is immediately in front of the upstream face of the weir, the second at its upstream edge and the third behind its downstream face. The most significant from the point of view of the capacity of the weir is the second zone of flow separation, which is discussed below in the text.

The second zone of flow separation (referred to hereinafter as the separation zone) is created immediately behind the upstream edge of the weir where the flow is separated to form the separation zone (*Hall*, 1962; *Bos*, 1989). In it, various non-stationary eddy structures are created, which influence the separated flow, causing, among others, also pulsation of the water surface (*ČSN ISO 3846*, 1994). Pulsation of the water surface is shown particularly in flow with separation. But it is also manifested, however, downstream, hence influencing, e.g., loading of the stilling basin, and partially also upstream, hence it can affect the water surface level at the profile of measurement for determining the overflow head h (Profile 1 at Fig. 1). Pulsation of the pressure p acts on the surface of the weir, which will cause oscillation of the weir and shortening of the lifetime of its surface (e.g. concrete). The existence of the separation zone reduces the capacity of the weir (*Tim*, 1986).

The measure for suppressing all of the above-given adverse effects is to eliminate the separation zone. This is achieved above all by the circular

curving of the upstream edge of the relative radius $r/P_1 \geq 0.25$ (*Tim*, 1986), or $r/h \geq 0.2$ at $t/h \geq 1.75$ and at the same time at $(t+r)/h \geq 2.25$ (*ČSN ISO 4374*, 1997), but also in other ways (*Hall*, 1962; *Raju* et al., 1977; *Noori* and *Juma*, 2009). The construction of the weir is thus affected and hence the requirements for its design will rise.

The knowledge of the shape of the separation zone and its behaviour is necessary in relation to the possible increase of the capacity of the weir and the removal of undesirable effects caused by flow separation.

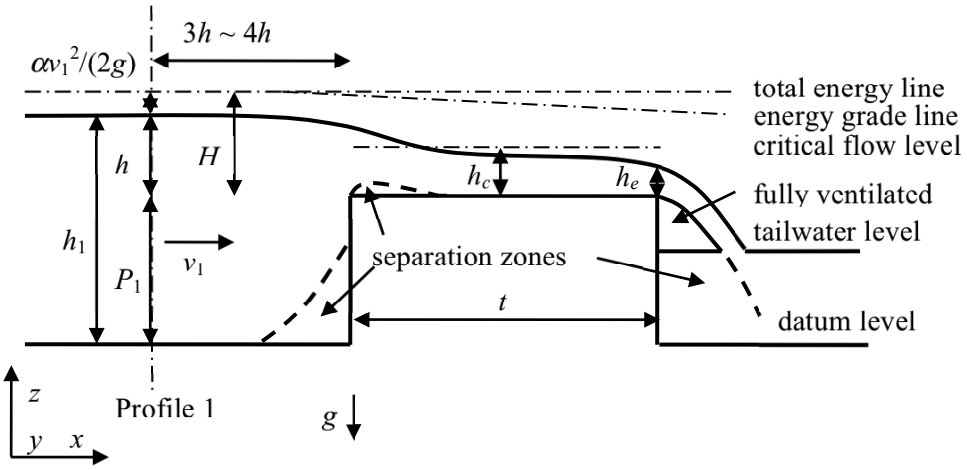

Fig. 1. Conditions of the free overfall of a rectangular broad-crested weir.

Characteristics of flow at the weir crest

The character of flow at the crest of a rectangular weir with free overfall is particularly dependent on the ratio of the energy overflow head to the weir thickness H/t, which is the relative thickness of the weir, and also on the ratio of the overflow head to the depth in front of the weir h/h_1 (*Bos*, 1989), or to the ratio relative to the weir height h/P_1 (*ČSN ISO 3846*, 1994), which is the relative height of the weir. Based on the ratio H/t, weirs are divided into: sharp-crested $1.5\ (1.8) < H/t$, short-crested (narrow-crested) $0.33\ (0.40) < H/t < 1.5\ (1.8)$, broad-crested $0.08 < H/t < 0.33\ (0.40)$ and long-crested $H/t < 0.08$ weirs (*Bos*, 1989; *Tim*, 1986; *Azimi* and *Rajaratnam*, 2009). In case of sharp-crested weirs, the separation zone is not created because the space beneath the nappe is filled by air (*Hager*, 1986). In case of short-crested weirs, the separation zone is created and has no similar geometry to the extent of its determination (H/t) because the character of flow near the separation is also changing (*Bos*, 1989); it depends both on the ratio H/t and the ratio h/h_1. In case of high broad-crested weirs in which $h/P_1 < 0.15$ (*ČSN ISO 3846*, 1994) or $h/h_1 < 0.35$ (*Bos*, 1989), when it approximately holds that $H = h$, the shape of the separation zone does not change (*Bos*, 1989); in lower broad-crested weirs it is assumed that its shape depends on the relative height of the weir h/h_1 (*Hall*, 1962). This paper is further concerned only with the separation zone during free overfall over broad-crested weirs in which $0.08 < H/t < 0.40$.

At the broad crest of a rectangular weir, subcritical flow changes to supercritical flow to form critical flow (*Clemmens* et al., 2001). Critical flow is characterized by the critical depth h_c, being for a rectangular cross section

$$h_c = \left(\frac{\alpha_c Q^2}{g b^2} \right)^{1/3}, \tag{1}$$

where α_c is the kinetic energy coefficient (it is further assumed that $\alpha_c = 1$), Q – the discharge, g – the acceleration of gravity and b is the width of the weir.

Shape of the water surface

Based on the investigation of flow, certain basic characteristics of the shape of the water surface have been identified at the weir crest, which are related either to the energy overflow head H, or to the overflow head h, or to the critical depth h_c (Fig. 2).

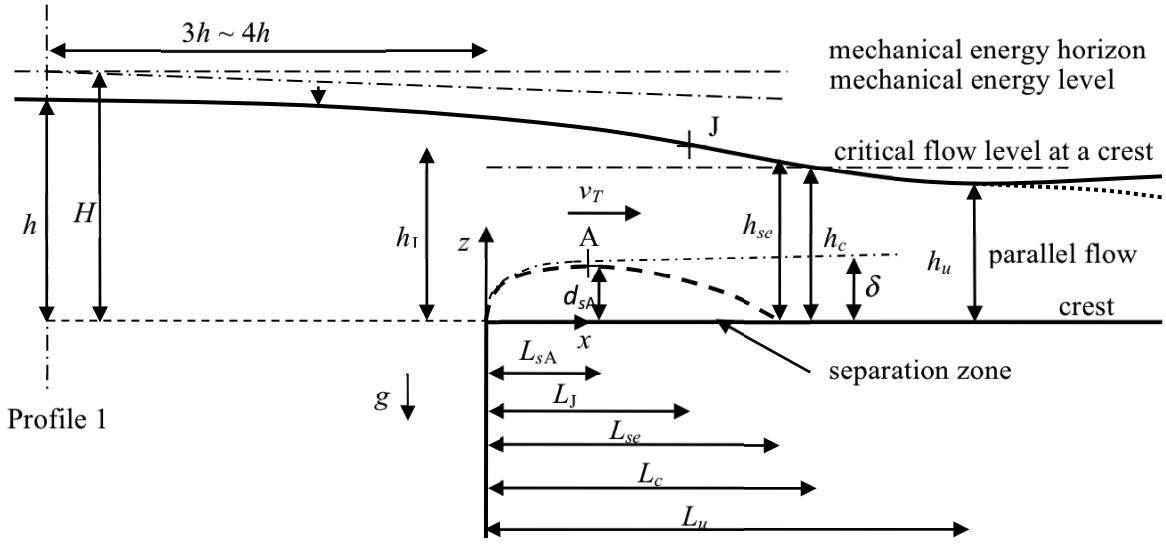

Fig. 2. Depiction of variables at the site of the separation zone.

The profile for water surface measuring to determine the overflow head h, that indicated the beginning of decreasing of the water surface caused by overflow, is at the distance $2h$ upstream in front of the weir (*Tim*, 1986). The standard (*ČSN ISO 3846*, 1994) recommends that the water surface level be measured at the distance $3h$ to $4h$.

The ratio of the critical depth to the energy overflow head is $h_c/H = 0.62$ (*Kolář* et al., 1983), or to the overflow head is $h_c/h = 0.60$ to 0.62 (*Tim*, 1986).

The profile with the critical depth L_c (Fig. 2) is approximately at the end of the separation zone $L_{se}/H = 1$ (*Hall*, 1962), where the relative depth is $h_{se}/H = 0.60$ (*Moss*, 1972). Downstream, approximately from the relative distance $L_u/h \approx 2$ (*Kolář* et al., 1983), $L_u/h \approx 3$ (*Tim*, 1986), flow is supercritical, approximately parallel, with the constant relative depths $h_u/H = 0.45$ (*Moss*, 1972), $h_u/H = 0.51$ (*Kolář* et al., 1983), $h_u/h = 0.44$ (*Tim*, 1986), $h_u/H = 0.46$ (*Hager* and *Schwalt*, 1994), and $h_u/h = 0.53$ at $H/t = 0.24$ (*Sarker* and *Rhodes*, 2004).

The shape of the water surface up to the profile of parallel flow is approximately symmetrical to the point J (Fig. 2), which is on the water surface at the relative level $Z_J = h_J/H = 0.73$ and at the relative distance $X_J = L_J/H \approx 2/3$ (*Hager* and *Schwalt*, 1994). The shape of the water surface $Z_h = z_h/H$, $X = x/H$ can be expressed dimensionless using the following equation (*Hager* and *Schwalt*, 1994)

$$\frac{Z_h - Z_{hJ}}{1 + c_J - Z_{hJ}} = \mathrm{tgh}\left(X_J - X\right), \tag{2}$$

where, in a range of $-1 < X < 2$, the correction coefficient is $c_J = 0.03$, otherwise it is $c_J = 0$.

In case of relatively very broad crests (only within the range of broad-crested weirs), the length of parallel flow is so large that its depth increases downstream due to the effect of friction on the surface of the weir (Fig. 2, solid line). The slope of the water surface depends on the roughness of the surface of the weir crest and its shape is determined, e.g., by the standard-step method. In case of relatively narrower crests (only within the range of broad-crested weirs), where the length of parallel flow is small, the depth is approximately constant, or decreases due to the closeness to the end depth (Fig. 2, dotted line).

Near to the downstream edge of the weir crest (end edge), the depth decreases due to the curvature of streamlines during free overfall down to the end depth h_e, which is relatively expressed as $h_e/H = 0.46$ (*Kolář* et al., 1983) and $h_e/h = 0.42$ (*Tim*, 1986). The ratios apply to the roughness of the surface of the weir manufactured from the materials mentioned above in the introduction to this paper.

Pressure in flow and on the surface of the weir

Due to flow separation behind the upstream edge of the weir, pressure relative to hydrostatic pressure is reduced in the separation zone. During the reattachment of the separated flow, pressure increases on the surface of the weir crest. The pressure field in parallel flow corresponds to the hydrostatic field (*Bos*, 1989).

Measurement of the pressure head $p/(\rho g)$, where ρ is the density of the liquid, was studied by *Moss* (1972), who expressed it relatively against the energy overflow head H for separated flow as well as for the separation zone. For the boundary of the separation zone, he determined an approximately constant value of $p/(\rho gH) = 0.60$ to 0.61. From the upstream edge of the weir crest up to the half-length of the separation zone, he determined a range of values of $p/(\rho gH) = 0.56$ to 0.58. The maximum value of the relative pressure head $p/(\rho gH) = 0.69$ was at the end of separation.

Based on measurement, *Tim* (1986) determined the pressure head $p/(\rho g)$ at the crest and on the upstream face of the weir. Behind the upstream edge of the weir, he obtained values in a range of $p/(\rho gh) = 0.54$ to 0.58. The maximum value was $p/(\rho gh) =$ 0.67 to 0.68.

Pressure on the surface of the upstream face and of the weir crest with using a manometer was measured by *Hager* and *Schwalt* (1994). Behind the upstream edge of the weir crest, they obtained the value $p/(\rho gH) = 0.56$ to 0.57 and the maximum value $p/(\rho gH) = 0.73$ was at the distance $x/H =$ 1.05.

Velocity field of flow

The velocity field at the weir crest is influenced by the formation of a boundary layer (*Hall*, 1962). The thickness δ of the boundary layer expressed relatively as δ/H increases downstream and depends on the value of the Reynolds number Re_H

$$\mathrm{Re}_H = \frac{v_T H}{\upsilon}, \tag{3}$$

which is expressed by the mean velocity v_T of separated flow (Fig. 2) and the kinematic viscosity υ.

Measurement of the velocity field of flow using a Pitot cylinder was made by *Moss* (1972). This measurement was made in points in verticals spaced at $x/H = 1/6$ in a range of $0 < x/H < 1$ and also spaced at $x/H = 1/3$. Only the velocity field of separated flow is evaluated, in the form of 76 vectors of point velocities. The velocity field in the separation zone was not evaluated due to the high degree of turbulence.

Measurement of velocities in the separation zone for two discharge stages using a miniature propeller meter was made by *Hager* and *Schwalt* (1994). They measured time-mean longitudinal point velocities u_x along a height with 10 mm spacing in selected verticals $x/H = -0.5, 0, 0.5, 1, 2$ and expressed the velocity field as the root of the ratio of the velocity head to the energy overflow head: $u_x/(2gH)^{1/2}$.

Shape of the separation zone

The separation zone forms immediately at the upstream edge of the weir crest (*Bos*, 1989). There, flow separates and re-attaches to the surface of the weir crest at the distance L_s, which is the length of the separation zone. The boundary between the separation zone and the separated flow is not clear because non-stationary eddies form there, delineating the sub-zone of turbulent mixing (*Moss*, 1972). The sub-zone of turbulent mixing widens downstream along the length of the boundary between the separation zone and the separated flow.

The approximate relative length of the separation zone in high weirs is $L_{se}/H = 1.0$ (*Hall*, 1962), $L_{se}/H = 1.4$ (*Moss*, 1972), $L_{se}/H = 1.18$ (*Hager* and *Schwalt*, 1994). Its length is determined with much difficulty because the boundary of separation is time-variable and depends on the Reynolds number Re_H (*Hall*, 1962).

The relative maximum thickness of the separation zone in high weirs is $d_{sA}/H \approx \delta^*/H = 0.109$ (Fig. 3, point A) at the relative distance $L_{sA}/H =$ $= 0.25$ (*Hall*, 1962); and $d_{sA}/H = 0.15$ (*Moss*, 1972), $Z_{sA} = d_{sA}/H = 0.20$ at the relative distance $X_A =$ $= L_{sA}/H = 0.44$ (*Hager* and *Schwalt*, 1994). The relative maximum thickness does not depend on the Reynolds number Re_H (*Hall*, 1962).

In lower weirs, the relative length and thickness of the separation zone also depends on the relative overflow head H/P_1 (*Hall*, 1962).

Hager and *Schwalt* (1994) express the shape of the boundary of the separation zone using the equation (here, it is modified and applies to the above-given Z_{sA} and X_A)

$$Z_s = -\frac{Z_{sA}}{X_A} X \ln\left(\frac{X}{e X_A}\right). \tag{4}$$

Hall (1962) expresses the shape of the separation zone using the displacement thickness δ^*. He states that it consists of three parts, the shape of which is described in Fig. 3.

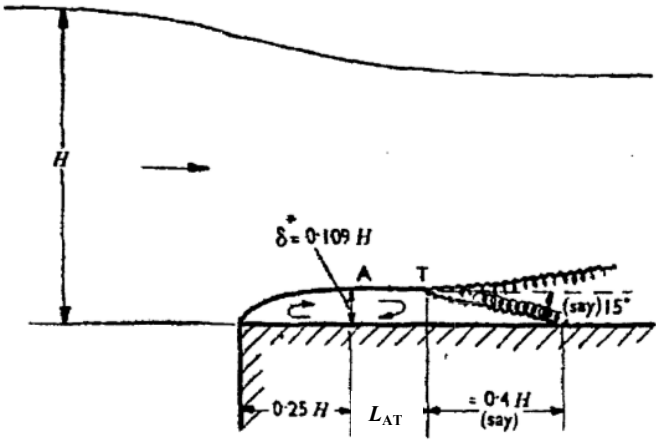

Re_H	L_{AT}/H
1 000	20
10 000	2
50 000	0.4
100 000	0.2

Fig. 3. Assumed structure of the separation zone as a function of the energy head H over the weir and the Reynolds number Re_H for high weirs $h = H$ (*Hall*, 1962).

Numerical modelling of overflow over a rectangular broad-crested weir

Some of the above-given ratios and equations, which were determined on the basis of measurement, were used for the verification of different methods of calculations of overflows over a rectangular broad-crested weir.

Moss (1972) determined the ratio $h_c/H = 0.60$ to 0.61 using $h_u/H = 0.45$, on the basis of 2D calculation using Laplace's equation and Bernoulli's equation for specifying the velocity at the boundary of the separation zone.

Sarker and *Rhodes* (2004) determined $h_u/h = 0.55$ (at $H/t = 0.24$) on the basis of 3D calculation using Reynolds-averaged Navier-Stokes (RANS) equations, a k-ε model of turbulence and Volume-of-Fluid (VOF) analysis.

Bombardeli with his colleagues (*Bombardeli* et al., 2000) made a 2D testing calculation of flow over a broad crest in an experiment published by *Hager* and *Schwalt* (1994), in which they used RANS equations, the re-normalisation group k-ε (RNG) model of turbulence and VOF analysis, and focused on the comparison of velocity fields, which were credibly simulated, and discharge, which differed from measurement by 3.1 %.

Hargreaves with his colleagues (*Hargreaves* et al., 2007) was concerned in detail with 2D and 3D numerical modelling of flow over a broad-crested weir. The used RANS equations and three models of turbulence: a standard k-ε, a RNG and a Reynolds stress model (RSM). For verifying the suitability of the model of turbulence, they used data determined from measurement (*Hager* and *Schwalt*, 1994). They focused, among others, on the agreement of the shape of the water surface, discharge, pressure at the weir crest and the range of the separation zone. The largest differences in the description of flow were recorded in the range of the separation zone. They state that the RNG and RSM models of turbulence yield a better agreement than the standard k-ε model.

Hsu and *Ozdemir* (2007) modelled the same problem and concentrated on the comparison of RNG and RSM models of turbulence. They state that the RSM model yields better results for the position of the water surface.

Evaluation of the current state

The above-given overview shows that certain characteristics of flow determined from measurement at the weir crest are not uniformly interpreted and the character of flow in the separation zone is not yet determined in detail experimentally. Experimentally determination of the flow separation enable makes validation tests of numerical models in higher quality, or design constructions directly on the basis of dimensionless characteristics of flow.

Experiment

An experiment was conducted in the Laboratory of Water Management Research of the Institute of Water Structures at the Faculty of Civil Engineering of the Brno University of Technology. A rectangular oblong broad-crested weir manufactured from plexiglass was mounted in a 1-m-wide and 12-m-long flume of a square profile, with glass side

walls and a concrete bottom, with an oblong glass visor of 0.39 m and 0.54 m in dimensions. The weir has the height $P_1 = 0.250$ m, its width was the same as the flume, i.e. $b = 1.003$ m, and the thickness was $t = 0.500$ m. It was mounted 2 m upstream from the end of the flume.

Water discharges Q were determined by measuring water surface levels in a measuring tank fitted with a calibrated Thomson weir. The range of discharges Q was from 0.010 m^3 s^{-1} to 0.130 m^3 s^{-1}. The inflow of water to the broad-crested weir was even, which was confirmed by the constancy of the velocity field along the length of flow upstream in front of the weir. Measurements of instantaneous point velocities U were made there using a UVP Monitor XW-Psi with 4MHz probes. The kinetic energy coefficient was determined at about $\alpha = 1.04$ from velocity fields. There was no access of air into the second separation zone. The outflow was free, the tailwater level did not influence overflow. The air pocket below the lower nappe was properly ventilated.

Water surface levels were measured in a longitudinal plane of the symmetry of the flume using a needle gauge fastened to a travel gear. They were also measured in selected cross profiles to confirm that they are not influenced by cross waves in the longitudinal plane of symmetry. Due to the above-given circumstances and in relation to the extent of the values of the ratios of the flume width to the overflow head $5 < b/h < 28$, flow in the longitudinal plane of symmetry can be considered as approximately two-dimensional. The relative thickness of the weir was in a range of $0.07 < h/t < 0.38$, which practically characterizes broad-crested weirs. The relative weir heights varied in a range of $0.14 < h/P_1 < 0.77$, which reaches also the area of high weirs. The overflow heads were in a range of 0.036 m $< h <$ 0.192 m, i.e. the requirement for the minimum overflow head $h_{min} = 0.06$ m (*ČSN ISO 3846*, 1994), (*Bos*, 1989), was not met only in discharges to 0.022 m^3 s^{-1} or to the discharge 0.016 m^3 s^{-1} for $h_{min} = 0.05$ m (*Hager* and *Schwalt*, 1994). The range of measurement of water surface levels downstream was -1.0 m $< x <$ 0.5 m, where the upstream edge of the weir was the beginning. The measured water surface levels z_h at the weir crest are depicted in Fig. 4.

Measurement of pressure heads $p/(\rho g)$ at the weir crest was made using piezometric holes connected with a tube panel in which water surface levels were measured and read out from the weir crest level. The measured pattern of pressure heads z_p is depicted in Fig. 4.

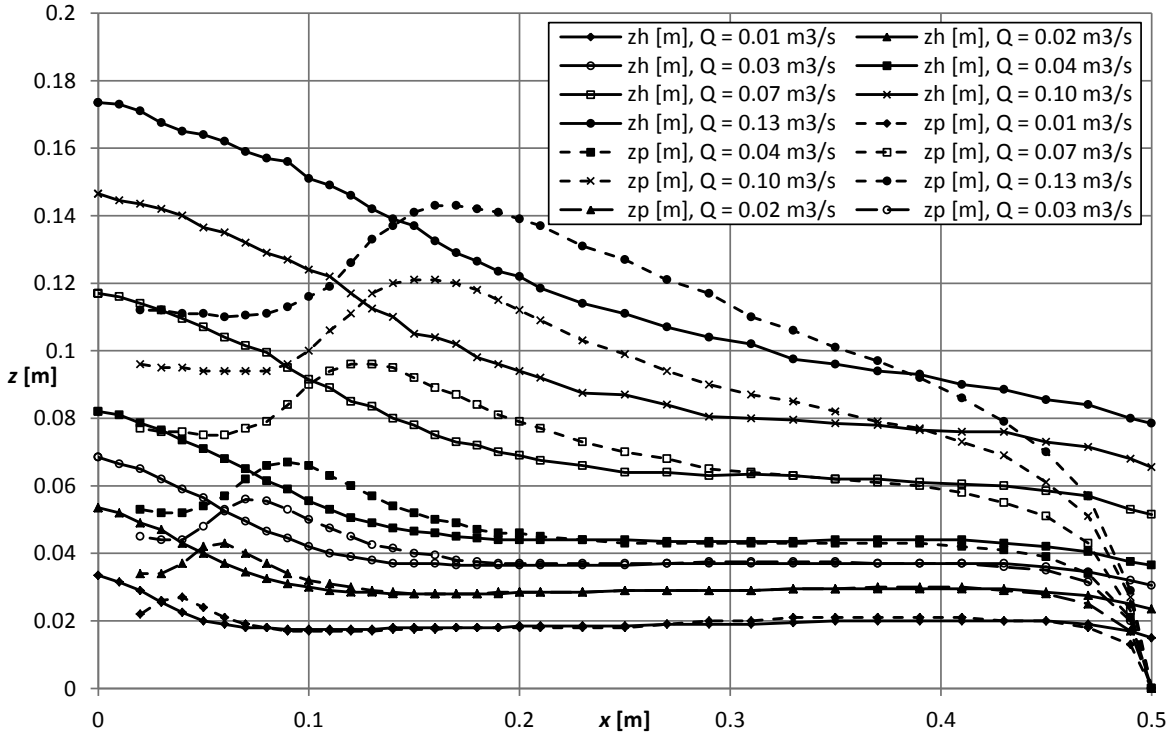

Fig. 4. Measured pattern of the water surface level z_h and the pressure head level z_p on the surface of the weir crest.

Measurements of velocity fields were made by Particle Image Velocimetry (PIV), a contactless laser method of measurement, with the use of the set Dantec FlowMap. In relation to the extent of the area of interest (the separation zone and the separated flow), the measurements were made in subparts with variable detail, highlighting the description of the velocity field in the separation zone. The sub-fields of instantaneous point velocities U were measured with a frequency of 2 Hz (in selected cases also with a frequency of 15 Hz) and a number of 100 measurements. They were used to determine the sub-fields of time-mean point velocities u and their fluctuations u'. The total fields were obtained by making up all respective sub-fields of time-mean point velocities and fluctuations with a priority (in overlapping zones) of the use of more detailed measurements. The measurements were made for the discharges 0.01, 0.04, 0.07, 0.10 and 0.13 $m^3 s^{-1}$.

Evaluation

Water surface level

The water surface level was evaluated dimensionless relative to the energy overflow head, i.e. $Z_h = z_h/H$ a $X = x/H$ (Fig. 5) with the beginning in the upstream edge of the weir crest and with the downstream orientation of the positive X-axis. It was also evaluated relative to the overflow head h ($H = h + \alpha v_1^2/(2g)$) and to the critical depth h_c. The conversion between the critical depth h_c and the energy overflow head H is made using the discharge coefficient C_D related to H which is a function of H/P_1, i.e.

$$h_c = \frac{2}{3} C_D^{2/3} H \,. \tag{5}$$

The shape of the water surface up to the profile of parallel flow is approximately symmetrical to the point J (Fig. 2), as given by *Hager* and *Schwalt* (1994). The best agreement of the water surfaces downstream up to the profile of the critical depth h_c is in relation to the overflow head h, and farther on in relation to the energy overflow head H. This is caused by the effect of the velocity head $\alpha v_1^2/(2g)$, which creates a change in the water surface level in front of the weir; its relative expression is $\alpha v_1^2/(2gH)$. Conversely, the depth of the parallel flow h_u is based on the energy overflow head H. Therefore, Eq. (2) was modified into a formula that contains the relative velocity head. In addition, step changes in the water surface level were eliminated by using the correction coefficient c_J differently. The modified Eq. (2) has then the formula

$$\frac{Z_h - Z_{hJ}}{1 - \dfrac{\alpha v_1^2}{2gH} - Z_{hJ}} = \mathrm{tgh}\left[c_J \left(X_J - X \right) \right], \tag{6}$$

where

$$Z_{hJ} = 0.5 \left(1 - \frac{\alpha v_1^2}{2gH} + Z_{hu} \right). \tag{7}$$

According to the measurement, $Z_{hu} = h_u/H = 0.47$ and $X_J = 0.67$ (for the highest ratios H/P_1 the values of Z_{hu} and X_J are smaller by 0.01, for the lowest ratios the values are larger by 0.01), and according to the analysis of the shape of the water surfaces using the method of least squares, $c_J = 1.20$. The extent of the validity of Eq. (6) is from the profile with the beginning of water surface curvature up to the profile with approximately parallel flow, i.e. $-2.0 < X < 2.7$.

The relative water surface level in the profile of the critical depth $Z_{hc} = h_c/H = 0.60$ is in the relative distance $X_c = L_c/H = 1.15$ (for the highest ratios H/P_1 the values of X_c are smaller by 0.02, for the lowest ratios the values are larger by 0.02).

The relative water surface level of approximately parallel flow at the weir crest for $H/t < 0.16$ (plexiglass) from the profile $X_u = L_u/H = 2.7$, where the water surface level is Z_{hu}, increases downstream due to the friction of flow on the weir surface. It increases up to the value $Z_{hm} = h_m/H$, or $Z^*_{hm} = h_m/h_c$ ($Z_{hm} = Z^*_{hm} h_c/H$) in the profile $X^*_m = l_m/h_c = -4.0$ (explained below), where the effect of overflow with the end depth h_e starts to be shown. The roughness coefficient $n = 0.009$ for the measured pattern of the water surfaces was determined iteratively by applying the standard-step method (*Kolář* et al., 1983) and with neglecting the effect of local losses. The value of coefficient corresponds to the values recommended in the professional literature (*Kolář* et al., 1983) for plexiglass. This shows that the given method is suitable for determining Z_{hm}, or Z^*_{hm}.

Hydraulic conditions affected by free overflow over the end edge is expressed the best in relation to the critical depth h_c, then the coordinate system is $Z^* = z/h_c$, $X^* = x^*/h_c$ with the origin in the end edge and the positive X^*-axis (x^*-axis) is in the di-

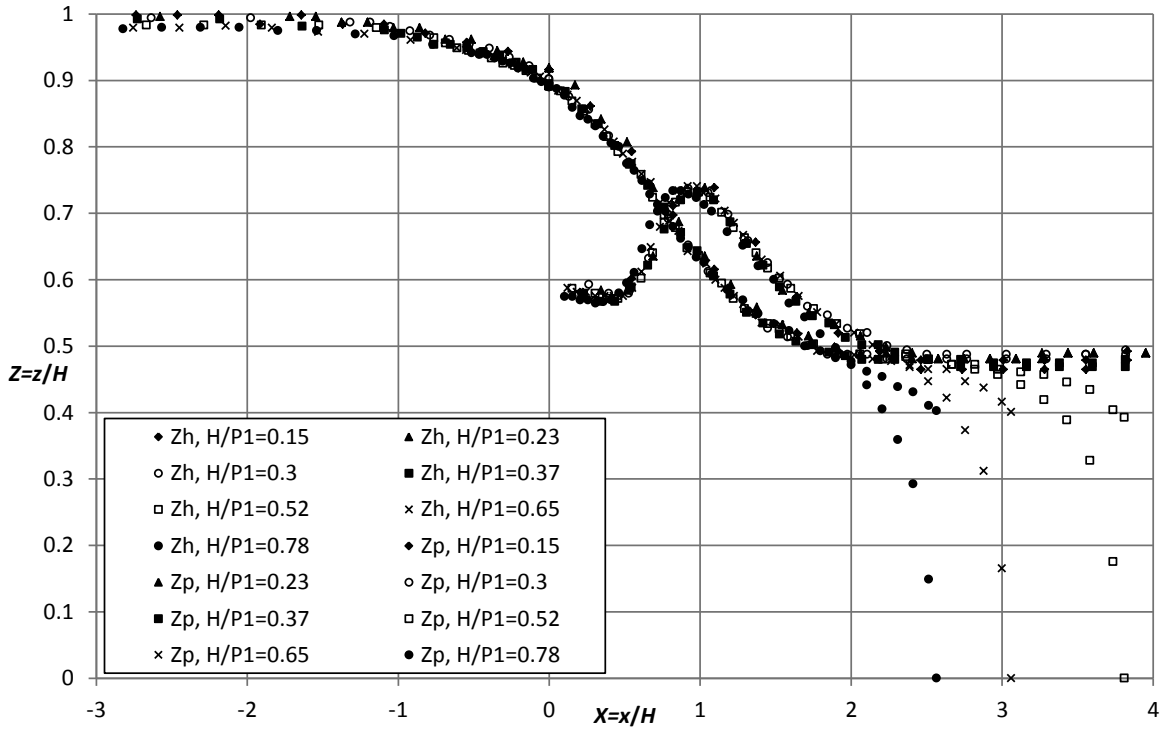

Fig. 5. Dimensionless expression of the position of the water surface Z_h and the pressure head Z_p in a range of $-3 < X < 4$.

rection of flow ($Z = Z^* h_c/H$, $X = X^* h_c/H$). For $H/t < 0.16$ the relative depth $Z^*_{hm} = h_m/h_c$ is approximately constant in a range of $-4.0 < X^* < -2.5$. Closer to the downstream edge ($-2.5 < X^*$), the relative depth gradually decreases down to the relative end depth $Z^*_{he} = h_e/h_c$. For $H/t > 0.16$, it is $h_u = h_m$, then also $Z^*_{hu} = Z^*_{hm}$. The relative end depth is a function of the Froude number $Fr_m = Q/(h_m^{3/2} b g^{1/2})$ determined for the depth h_m (h_u) (*Davis* et al., 1998); the measurement ($R^2 = 0.91$) shows that

$$Z^*_{he} = \frac{h_e}{h_c} = 0.8443 - 0.1297\,\mathrm{Fr}_m\,. \tag{8}$$

The shape of the water surface in a relative length range of $-2.5 < X^* < 0.0$ can be expressed by the equation

$$\frac{Z^*_h - Z^*_{he}}{Z^*_{hm} - Z^*_{he}} = \mathrm{tgh}\left(-X^*\right). \tag{9}$$

In the case of flow when there is an overlap between the extent of validity of Eq. (6) and Eq. (9), it is possible to approximate the shape of the water surface level in the overlap of validities by a line segment which is tangent (if possible) to both the curves expressed by the given equations.

Pressure head at the weir crest

The time-mean values of pressure heads were plotted relative to the energy overflow head H, i.e. $Z_p = p/(\rho g \mathrm{H})$ (Fig. 5), and also to the overflow head h and the critical depth h_c. The best agreement of their levels, not their positions, is in the expression relative to the energy overflow head H. Its mean shape is characterized by the following equations:
In a range of $0.10 < X < 0.65$, the equation ($R^2 = 0.78$) is

$$Z_p = \frac{z_p}{H} = 1.1154X^3 - 0.8181X^2 + 0.1504X + 0.5728, \tag{10a}$$

in a range of $0.65 < X < 1.30$, the equation ($R^2 = 0.86$) is

$$Z_p = \frac{z_p}{H} = 1.0702X^3 - 3.9632X^2 + 4.6136X - 0.9896, \tag{10b}$$

and in a range of $1.3 < X < 2.7$, the equation ($R^2 = 0.98$) is

$$Z_p = \frac{z_p}{H} = -0.0403X^3 + 0.348X^2 - 1.0205X + 1.4875. \quad (10c)$$

For the largest values it is necessary to shift the whole pattern by the value $X = -0.05$, for the smallest values of H/P_1 by the value $X = 0.05$.

In a range of $X = 2.7$ to $X^* = -2.5$, it is $Z_p = Z_h$. In a range of $0.0 > X^* > -2.5$, Z^*_p is determined by the equation

$$Z^*_p = \frac{Z^*_{hm}}{Z^*_{hc}} \text{tgh}\left[1.4\left(-X^*\right)^{0.6}\right]. \quad (11)$$

In the case of flow when there is an overlap between the extent of validity of Eq. (10c) and Eq. (11), it is possible to approximate the shape of the pressure curve level by a segment line which is tangent (if possible) to both the curves expressed by the given equations.

Velocity head

The velocity fields were expressed dimensionless as the velocity head related to the energy overflow head $u^2/(2gH)$. The shape of the velocity field depends on the relative weir height H/P_1. For its visualisation, which is depicted in Fig. 6, the mean field was plotted in the form of mean contours at all of the measured stages H/P_1.

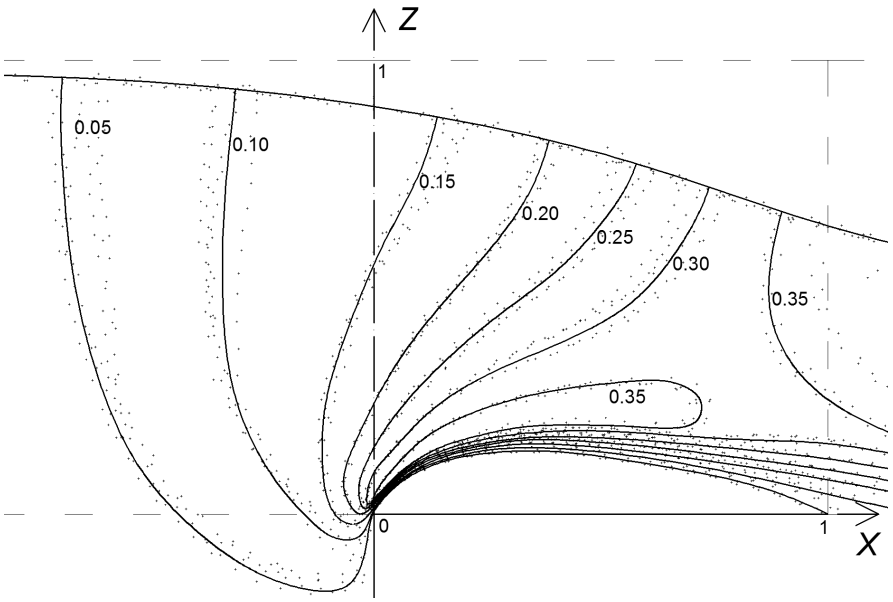

Fig. 6. Dimensionless expression of the velocity head $u^2/(2gH)$ of flow in a range of $-0.5 < X < 1.0$.

The mean position Z_{vmax} of the curve with the maximum value of the time-mean point velocity along the length of flow was evaluated in a range of $0.0 < X < 0.8$ ($R^2 = 0.99$)

$$Z_{v\max} = 1.618X^3 - 2.318X^2 + 1.120X + 0.036. \quad (12)$$

Boundary of the separation zone

The boundary of the separation zone was determined on the basis of the evaluation of the time-mean vector fields of velocity. The flow fields were described using the trajectories of particles by means of the program SMS 11, from which the level Z_s of the boundary of the separation zone was generated and is described by Eq. (4) in a range of $0.00 < X < 0.38$ with $X_A = 0.38$ and ($R^2 = 0.98$)

$$Z_{s\text{A}} = -0.0307\left(\frac{H}{P_1}\right)^2 + 0.0103\frac{H}{P_1} + 0.164. \quad (13)$$

For $X > 0.38$ up to the distance ($R^2 = 0.95$)

$$X_e = \frac{L_{se}}{H} = -0.1203\frac{H}{P_1} + 0.8735, \quad (14)$$

the shape of the boundary of the separation zone is determined by the equation

$$\frac{\left(Z_s - c_s\right)^2}{\left(Z_{s\mathrm{A}} - c_s\right)^2} = 1 - \frac{\left(X - X_\mathrm{A}\right)^2}{\left(X_e - c_e - X_\mathrm{A}\right)^2}, \qquad (15)$$

where $c_s = -0.04$ and $c_e = -0.01$ are correction coefficients.

Turbulence

The curve representing the maximum value of turbulence kinetic energy along the length of flow copies the boundary of the separation zone in a range of $0.00 < X < 0.38$. In a range of $0.38 < X < 0.65$, the curve with the maximum value of turbulence intensity is lower by up to $\Delta Z = 0.01$ in 2/3 of the given range than the boundary of the separation zone. Also, the curves intersect at the level $Z_s = 0.10$ and gradually pass to the approximately constant level $Z_s = 0.06$ at the distance $X = 1$ (the velocity field has not been further evaluated).

For the description of the shape of the time-mean eddy in the separation zone, the curve $u_x^2/(2gH) = 0$ was also evaluated, with its level Z_{vx0} in a range of $0.0 < X < 0.6$ being described by the equation ($R^2 = 0.98$)

$$Z_{vx0} = -3.684X^4 + 6.35X^3 - 4.067X^2 + 1.062X + 0.005. \qquad (16)$$

The curve continues farther ($X > 0.6$) in relationship to the relative weir head H/P_1 up to $Z_{vx0} = 0$ at the distance X_e of the given Eq. (14).

Evaluation

Based on the evaluation of measurement dimensionless relative to the energy overflow head H to the distance $X = 2.7$, the basic characteristics of flow at the crest of a rectangular broad-crested weir are described. These are particularly the determination of the water surface level, the pressure head level on the surface of the weir crest, the mean velocity head (to $X = 1.0$), the level of the boundary of the separation zone, the level of the curve with the maximum value of turbulence kinetic energy along the length of flow (to $X = 0.6$) and the level of the curve with zero x-velocity in the separation zone. Also, an approach to the determination of the water surface level and the level of the pressure head curve of approximately parallel flow at the weir crest is shown and verified. And, subsequently, the water surface level and the pressure head curve level on the surface of the weir crest are described dimensionless relative to the critical depth h_c from the distance $X^* = -3$.

The results evaluated from the new detailed measurements specify and extend certain previous observations. These concern particularly the characteristics of flow in the separation zone, which could not have been measured in detail in the past. The results will also enable the validation of numerical models of flows, particularly their models of turbulence. They will also enable a more effective design of constructions without the necessity of numerical or physical modelling.

Research confirmed the values of discharge coefficient recommended for rectangular broad-crested weirs by standard (*ČSN ISO 3846*, 1994) over the whole range of measured values (*Zachoval* and *Roušar*, 2011).

Acknowledgements. Thanks are due to the project GA103/09/0977 – Experimental and numerical modelling of turbulent flow with massive separation and to the project FAST-S-11-59 – Experimental research and numerical modelling of flow separation behind the upstream edge of a broad-crested weir with a rectangular cross section.

List of symbols

b – channel width, weir width [m],
C_D – discharge coefficient,
c_J – correction coefficient,
c_s – correction coefficient,
c_e – correction coefficient,
$d_{s\mathrm{A}}$ – separation zone thickness in the profile with point A [m],
Fr_m – Froude number,
g – acceleration of gravity [m s^{-2}],
H – energy overflow head [m],
h – overflow head [m],
h_1 – depth of channel flow [m],
h_c – critical depth [m],
h_e – end depth [m],
h_J – depth in the profile with point J [m],
h_{se} – depth at the end of separation zone [m],
h_u – depth at the beginning of parallel flow [m],
L_{AT} – distance between points A and T [m],
L_J – distance of profile with point J [m],
L_c – distance of profile with critical depth [m],
$L_{s\mathrm{A}}$ – distance of profile with point A [m],
$L_{s\mathrm{e}}$ – length of separation zone [m],
L_u – distance of profile with parallel flow [m],
n – roughness coefficient,
Q – discharge [m^3 s^{-1}],
p – pressure [Pa],
P_1 – weir height [m],
R^2 – determination coefficient,
Re_H – Reynolds number related to H,
r – upstream corner radius of weir crest [m],
t – weir thickness [m],
U – instantaneous point velocity [m s^{-1}],

u – time-mean point velocity [m s^{-1}],
u_x – x-component of time-mean point velocity [m s^{-1}],
u_x' – fluctuation of instantaneous time-mean point velocity [m s^{-1}],
v_1 – mean flow velocity in the channel [m s^{-1}],
v_m – cross-sectional velocity at the end of parallel flow [m s^{-1}],
v_T – cross-sectional velocity of separated flow [m s^{-1}],
$X=x/H$ – dimensionless coordinate with origin at the upstream edge of weir crest,
$X^*=x/h_c$ – dimensionless coordinate with origin at the downstream edge of weir crest,
x – coordinate with origin at the upstream edge of weir crest [m],
$Z=z/H$ – dimensionless coordinate with origin at the upstream edge of weir crest,
$Z^*=z/h_c$ – dimensionless coordinate with origin at the downstream edge of weir crest,
Z_h – dimensionless water surface level,
Z_{hc} – dimensionless water surface level of critical flow,
Z_{hJ} – dimensionless water surface level in the profile with point J,
Z_{hm} – dimensionless water surface level at the profile with end of parallel flow,
Z^*_{hm} – dimensionless water surface level at the profile with end of parallel flow,
Z_{hu} – dimensionless water surface level in the profile with the beginning of parallel flow,
Z_p – dimensionless pressure head level,
Z^*_p – dimensionless pressure head level,
Z_s – dimensionless level of the boundary of separation zone,
Z_{sA} – dimensionless level of the boundary of separation zone in the profile with point A,
Z_{vmax} – dimensionless level of curve with maximal point velocity,
Z_{vx0} – dimensionless level of curve with zero x-component point velocity,
z – coordinate with origin at the upstream edge of weir crest [m],
z_h – water surface level [m],
α – kinetic energy coefficient,
δ – boundary layer thickness [m],
δ^* – displacement thickness of boundary layer [m],
ρ – density [kg m^{-3}],
υ – kinematic viscosity [m^2 s^{-1}].

REFERENCES

AZIMI A. H., RAJARATNAM N., 2009: Discharge Characteristics of Weirs of Finite Crest Length. J. Hydraul. Engng., ASCE.

BOMBARDELI F. A., GARCÍA M. H., CAISLEY M. E., 2000: 2-D and 3-D Numerical Simulation of Abrupt Transitions in Open-Channel Flows. Application to the design of canoe chutes. HydroInformatics 4th. Iowa Institute of Hydraulic Research.

BOS M. G., 1989: Discharge measurement structures. Third revised edition. Publication 20. ILRI. 1989. ISBN 90 70754 15 0.

BOITEN W., 2002: Flow measurement structures. Flow Measurement and Instrumentation 13. pp. 203–207. Elsevier.

CLEMMENS A. J., WAHL T. L., BOS M. G., REPLOGLE J. A., 2001: Water Measurement with Flumes and Weirs. International Institute for Land Reclamation and Improvement/ILRI, Wageningen, Netherlands.

ČSN ISO 3846 (25 9332), 1994: Liquid flow measurement in open channels by weirs and flumes. Rectangular broad-crested weirs.

ČSN ISO 4374 (25 9337), 1997: Liquid flow measurement in open channels. Round-nose horizontal broad-crested weirs.

DAVIS A. C., ELLET B. G. S., JACOB R. P., 1998: Flow Measurement in Sloping Channels with Rectangular free Overfall. J. Hydraul. Engng., pp. 760–763.

HAGER W., 1986: Discharge measurement structures. Ecole polytechnique Fédérale de Lausanne. Lausane.

HAGER W. H., SCHWALT M., 1994: Broad-Crested Weir. J. Irrig. Drain. Engng., Vol. *120*, ASCE.

HALL G. W., 1962: Analytical determination of the discharge characteristics of Broad-crested weirs using boundary layer theory. Proceedings of the Institution of Civil Engineers. Vol. *22*, No. 6607. pp. 177–190.

HARGREAVES D. M., MORVAN H. P., WRIGHT N. G., 2007: Validation of the volume of fluid method for free surface calculation: The broad-crested weir. Engng. Applicat. Comput. Fluid Mech., Vol. *1*, No. 2, pp.136–146.

HSU T., OZDEMIR E. C., 2007: Study of complex flows through SFWMD culvert structures by CFD modeling. Report as of FY2007 for 2006FL146B: "Complex flows through culvert structures by CFD modeling".

KOLÁŘ V., PATOČKA C., BÉM J., 1983: Hydraulics. (In Czech.) SNTL, Praha, 1983.

MOSS W. D., 1972: Flow separation at the upstream edge of square-edged broad-crested weir. J. Fluid Mech., Vol. *52*, part 2, pp. 307–320.

NOORI B. M. A., JUMA I. A. K., 2009: Performance Improvement of Broad Crested Weirs. Al-Rafidain Enging. Vol. *17*.

RAJU K. G. R., SHARMA S., KRISHNA S. M., 1977: Effect of Increase of Momentum on Discharge Characteristics of Broad-Crested Weirs. 6th Australian Hydraulics and Fluid Mechanics Conference. Adelaide, Australia.

SARKER M. A., RHODES D. G., 2004: Calculation of free-surface profile over a rectangular broad-crested weir. Flow Measurement and Instrumentat, 15. pp. 215–219.

TIM U. S., 1986: Characteristics of some hydraulics structures used for flow control and measurement in open channels. Concordia University. Montreal, Canada, p. 252. ISBN: 0-315-35552-2.

USBR, 2001: Water measurement manual. A water resources technical publication. U.S. Department of the Interior, Bureau of Reclamation. Third edition revised, reprinted 2001. 485 p. ISBN: 978-0160617638.

ZACHOVAL Z., ROUŠAR L., 2011: Discharge coefficient of rectangular broad-crested weir. (In Czech.) Sympózium Hydrotechnikov 2011. Slovak University of Technology in Bratislava. pp. 214–222. ISBN 978-80-227-3593-3.

Received 6 December 2011
Accepted 17 October 2012